

Diagnostic of Horndeski Theories

Louis Perenon, Christian Marinoni and Federico Piazza

Aix Marseille Univ, Université de Toulon, CNRS, CPT, Marseille, France.

Abstract

We study the effects of Horndeski models of dark energy on the observables of the large-scale structure in the late time universe. A novel classification into *Late dark energy*, *Early dark energy* and *Early modified gravity* scenarios is proposed, according to whether such models predict deviations from the standard paradigm persistent at early time in the matter domination epoch. We discuss the physical imprints left by each specific class of models on the effective Newton constant μ , the gravitational slip parameter η , the light deflection parameter Σ and the growth function $f\sigma_8$ and demonstrate that a convenient way to dress a complete portrait of the viability of the Horndeski accelerating mechanism is via two, redshift-dependent, diagnostics: the $\mu(z) - \Sigma(z)$ and the $f\sigma_8(z) - \Sigma(z)$ planes. If future, model-independent, measurements point to either $\Sigma - 1 < 0$ at redshift zero or $\mu - 1 < 0$ with $\Sigma - 1 > 0$ at high redshifts or $\mu - 1 > 0$ with $\Sigma - 1 < 0$ at high redshifts, Horndeski theories are effectively ruled out. If $f\sigma_8$ is measured to be larger than expected in a Λ CDM model at $z > 1.5$ then Early dark energy models are definitely ruled out. On the opposite case, Late dark energy models are rejected by data if $\Sigma < 1$, while, if $\Sigma > 1$, only Early modifications of gravity provide a viable framework to interpret data.

Contents

1	Introduction	2
2	Formalism: the effective theory of dark energy	4
2.1	Setting the background	5
2.2	Classifying dark energy models	5
2.3	Extracting observables	6
2.4	Viability criteria	8
3	General predictions on LSS observables	8
3.1	LDE scenario	9
3.2	EDE and EMG scenarios	10
4	Discussion	13
4.1	Constraining power of viability conditions	14
4.2	Effects of the background expansion history	14
4.3	Consistency and robustness checks	14
5	Conclusions	17
A	Parametrisation of the couplings	18
B	Links with the α-parametrisation	19

1 Introduction

Current and future observations aiming at understanding the nature of cosmic acceleration offer the unique possibility of testing predictions of general relativity (GR) on scales well beyond those of the solar system, where GR has received its most impressive confirmations. Upcoming galactic surveys such as DES [1], Euclid [2–4], DESI [5], LSST [6], WFIRST [7] and SKA [8–10] are expected to provide unprecedented datasets with which to investigate, in an accurate way, how structures form and grow, and how light rays bend in the presence of local gravitational potentials. Anticipating interesting signals of non-standard gravity that could be potentially detected by such future surveys of the large-scale structure (LSS) of the universe is a crucial task.

Any deviation from the standard Λ CDM paradigm will imply some anomalous relation among the curvature perturbation Ψ , the Newtonian potential Φ and the comoving density contrast of non relativistic matter Δ . These effects can be encoded in time and scale modifications to the effective Newton’s constant parameter μ and to the gravitational slip parameter η [11]. The former quantity describes how fluctuations of the matter fields interact in the universe, while the latter encapsulates non-standard relation between the Newtonian potential Φ (time-time part of the metric fluctuations) and the curvature potential Ψ (space-space part). From μ and η one can derive a further parameter, Σ , of more direct relevance for lensing surveys [12]. Σ relates the matter over-density with the lensing (or Weyl) potential $\Phi_+ = (\Phi + \Psi)/2$. Another convenient quantity to describe the gravitational clustering of matter is the product of the linear growth factor f and the *rms* density fluctuations on a scale of $8h^{-1}$ Mpc ($f\sigma_8$). This quantity, which can be optimally estimated from the analysis of the redshift space distortions

induced by the large-scale, coherent, in-falling(/out-flowing) of matter into(/out of) high(/low) density regions, is another key quantity turning galaxy redshift surveys into gravity probes.

While any observed deviation would represent a major discovery in itself, it is important to understand what type of signals are implied by concrete alternatives to the standard model and interpret them in terms of fundamental theoretical proposals. In particular, theories containing one extra scalar degree of freedom and leading to equations of motion of at most second order—*Horndeski theories* [13, 14]—despite the freedom in the choice of their free functions and the richness of their potential phenomenology, have proven to share common features and universal behaviours. On the one hand, the exclusion of pathologies and instabilities imposes tight constraints and well defined patterns for the time scaling of relevant observables of the LSS in the universe [15–17]. In particular, it was pointed out in [16] that the linear growth rate of Horndeski theories is systematically lower, at low redshift, than the value predicted by the standard Λ CDM model. On the other hand, the authors in [18] have argued that Horndeski theories are expected to display a systematic sign agreement in the μ - Σ plane across all cosmic epochs.

Investigating the existence of further general patterns displayed by LSS observables is the main goal of the present work. To this purpose, we present a complete study of the Horndeski phenomenology that generalizes in many respects that presented in [16]. First of all, we explore accelerating cosmologies in which the presence of dark energy is not confined to the late times [19–37]. At first sight, this is counter intuitive, as the acceleration is a recent phenomenon and there is no need to invoke dark energy effects at early times. Truth is that, although such effects are not needed, not to say wanted, they are allowed within the context of Horndeski theories, therefore they must be thoroughly investigated and systematised. In particular, we find convenient to highlight three possibilities of increasing generality.

- *Late-time dark energy (LDE)*: This is the reference class of models (explored at length in [16]), in which both the dark energy momentum tensor and the possible modifications of gravity (*i.e.* the non-minimal gravitational couplings) become negligible at early times.
- *Early dark energy (EDE)*: In these scenarios dark energy can contribute to the total energy momentum tensor even at early times, while non-minimal gravitational couplings are kept as a late-time phenomenon.
- *Early modified gravity (EMG)*: Horndeski theories in their full generality. Not only does dark energy always contribute to the total energy momentum tensor, but modified gravity effects are also persistent at early times, during matter domination.

On top of singling out the specific phenomenological features of the Horndeski sub-classes listed above, in this work we extend the analysis of [16] by including different background expansion histories than the Λ CDM model. Beside an effective equation of state parameter $w = -1$ (roughly, the value preferred by current observations, *e.g.* [38–40]), we also consider models with $w = -0.9$ and $w = -1.1$. In [16] it was found that viability priors do impose tight constraints and well defined patterns for the time scaling of relevant observables of the LSS in the universe. As such, viability criteria can be effectively used to complement data and observational information in statistical inferences. Testing the consequences of relaxing some of these restrictions is also a goal of the present study.

The main results of the paper are recapped in Figure 6 as exclusion regions in the parameter space of LSS observables. In the μ - Σ plane we highlight regions where the eventual presence of data would rule out the entire class of Horndeski theories. On the other hand, specific regions in the $f\sigma_8$ - Σ allow to rule out specific subclasses of models (LDE and/or EDE) presented above. A “complete diagnostic” of Horndeski theories is presented in the other figures of the paper.

The paper’s structure is as follows: in Sec. 2 we introduce the formalism adopted for the description of the background cosmic evolution, the non-minimal gravitational couplings and their relations with the LSS observables. In Sec. 3 we present our results in the case of a cosmic expansion history identical to that of Λ CDM, for the three classes of models described above. In Sec. 4 we verify the robustness of our conclusion by considering different equations of state for dark energy and by relaxing some of our viability conditions. The synthesis of our results as well as some digressions on future prospects are in Sec. 5.

2 Formalism: the effective theory of dark energy

The effective field theory of dark energy (EFT of DE) [41–47] proves a very powerful mean to explore the cosmological implications of Horndeski theories (see [48–51] for a numerical implementation of this formalism and [52–56] for generalizations to beyond-Horndeski and/or to models with non-minimally coupled dark matter). For such theories, the action up to second order in cosmological perturbations displays six functions of cosmic time,

$$S = S_m[g_{\mu\nu}, \psi_i] + \int d^4x \sqrt{-g} \frac{M^2(t)}{2} \left[R - 2\lambda(t) - 2\mathcal{C}(t)g^{00} - \mu_2^2(t)(\delta g^{00})^2 - \mu_3(t)\delta K\delta g^{00} + \epsilon_4(t) \left(\delta K_\nu^\mu \delta K_\mu^\nu - \delta K^2 + \frac{{}^{(3)}R\delta g^{00}}{2} \right) \right], \quad (1)$$

$M(t)$ is the “bare planck mass”, $\mathcal{C}(t)$ and $\lambda(t)$ are the contributions of the scalar field to the background energy momentum tensor, and $\mu_2^2(t)$, $\mu_3(t)$ and $\epsilon_4(t)$ are non-minimal couplings¹.

The Brans-Dicke subset of theories is characterized by a time-varying bare Planck mass $M(t)$, while all other non-minimal couplings are set to zero. A measure of the deviations from general relativity within the Brans-Dicke sector are more usefully defined by

$$\mu_1 = \frac{d \ln M^2(t)}{dt}. \quad (2)$$

One apparent feature of the above action is that the second line is quadratic in cosmological perturbations ($\delta K_{\mu\nu}$ being the perturbation of the extrinsic curvature of the hypersurfaces at constant scalar field value, and ${}^{(3)}R$ their intrinsic curvature. We refer the reader *e.g.* to the review [46] for more details), which means the first three operators uniquely govern the evolution of the background. Indeed, by varying the first line with respect to the metric one obtains the two equations

$$\mathcal{C} = \frac{1}{2} (H\mu_1 - \dot{\mu}_1 - \mu_1^2) - \dot{H} - \frac{\rho_m}{2M^2}, \quad (3)$$

$$\lambda = \frac{1}{2} (5H\mu_1 + \dot{\mu}_1 + \mu_1^2) + \dot{H} + 3H^2 - \frac{\rho_m}{2M^2}, \quad (4)$$

where a dot means a derivative with respect to cosmic time, $H(t) = \dot{a}/a$ is the Hubble parameter and only pressureless non-relativistic matter of energy density ρ_m has been assumed. Note that μ_1 is the only non-minimal coupling entering the background evolution. When μ_1 vanishes and $M = M_{\text{pl}}$, the above equations are particularly transparent, \mathcal{C} and λ play the role of the kinetic and potential term of a quintessence field respectively.

¹The coupling function μ_i have the dimension of mass and of order Hubble. μ_3 appears in cubic galileon and Horndeski-3 Lagrangians whereas ϵ_4 is a dimensionless order one function characterising galileon-Horndeski 4 and 5 Lagrangians.

2.1 Setting the background

The homogeneous background expansion history is characterised by the Hubble rate $H(t)$. We focus on models with a constant effective equation of state w_{eff} , *i.e.* those with a Hubble rate that scales as a function of the redshift as

$$\frac{H^2(z)}{H_0^2} = \Omega_{m,0}(1+z)^3 + (1 - \Omega_{m,0})(1+z)^{3(1+w_{\text{eff}})}, \quad (5)$$

where $\Omega_{m,0}$ is the present fractional matter density. Without direct relation with the EFT action (1), the above expression descends from a “standard” Friedmann equation

$$H^2 = \frac{1}{3M_{\text{Pl}}^2}(\rho_m + \rho_D^{\text{eff}}), \quad (6)$$

with $\rho_D^{\text{eff}} \propto a^{-3(w_{\text{eff}}+1)}$. As known, observations suggest $\Omega_{m,0} \sim 0.3$ and $w_{\text{eff}} \sim -1$ [39, 57]. In summary, our theories are defined, in their background and perturbation sectors, by two parameters and four functions of the time,

$$\{\Omega_{m,0}, w_{\text{eff}}, \mu_1(t), \mu_2^2(t), \mu_3(t), \epsilon_4(t)\}. \quad (7)$$

To characterise the evolution of the late time universe, we find convenient to use the fractional matter density of the background reference model (5) calculated at any epoch, x , as our time variable. Expressed as a function of the redshift it reads

$$x = \frac{\Omega_{m,0}}{\Omega_{m,0} + (1 - \Omega_{m,0})(1+z)^{3w_{\text{eff}}}}. \quad (8)$$

and its present day value is $x(t_0) \equiv x_0 = \Omega_{m,0}$.

2.2 Classifying dark energy models

In general, it is natural to *define* as in [42] the energy density of dark energy through the equation

$$H^2 = \frac{1}{3M^2}(\rho_m + \rho_D). \quad (9)$$

We note that, as opposed to the definition given *e.g.* in [53], here ρ_D does not depend on the matter fields, as much as, since we work in the Jordan frame, ρ_m is not a functional of the scalar field ϕ . We have now the instruments to define the three different general types of behaviour for dark energy at early times:

- **Late-time dark energy (LDE):** This is the minimal model, in which all effects of dark energy are confined to late times. Not only do non minimal couplings ($\mu_1, \mu_2^2, \mu_3, \epsilon_4$) go to zero at early times—which in the case of the coupling μ_1 implies M going to a constant—but also the dark energy density ρ_D becomes a sub-dominant component for $t \rightarrow 0$. In other words, the energy density of non relativistic particles ρ_m must saturate the Friedmann equations at early time. By comparing (6) and (9) this means that $M^2/M_{\text{Pl}}^2 \rightarrow 1$. In summary,

$$\text{LDE} : \left\{ \frac{M^2}{M_{\text{Pl}}^2} \rightarrow 1, \frac{\mu_1}{H} \rightarrow 0, \frac{\mu_2^2}{H^2} \rightarrow 0, \frac{\mu_3}{H} \rightarrow 0, \epsilon_4 \rightarrow 0 \right\}_{x \rightarrow 1}. \quad (10)$$

The above defined class of models generalises the set explored by [16]. Indeed, we allow the coupling μ_2^2 to be nonzero over most of cosmic history, *i.e.* for $x \neq 1$, and we also consider expansion histories different from that of a Λ CDM model, *i.e.* $w_{\text{eff}} \neq -1$.

- **Early dark energy (EDE)**: The dark energy contributes to the total energy momentum tensor even at early times, when, however, all non-minimal couplings vanish. The only way this is possible is for dark energy to acquire the same equation of state as dark matter early on, so that it becomes indistinguishable from the latter as long as the background evolution is concerned,

$$\mathbf{EDE} : \left\{ \frac{M^2}{M_{\text{pl}}^2} \rightarrow \text{const.}, \frac{\mu_1}{H} \rightarrow 0, \frac{\mu_2^2}{H^2} \rightarrow 0, \frac{\mu_3}{H} \rightarrow 0, \epsilon_4 \rightarrow 0 \right\}_{x \rightarrow 1}. \quad (11)$$

A caveat must be issued regarding the use we make of the adjective “early”. Our study is oblivious of the radiation dominated epoch. Therefore “early” for us means always well after equivalence, say, at $z \simeq 100$ but well before the onset of acceleration, at $z \simeq 1$.

- **Early modified gravity (EMG)**: This is the most general case. Here we allow also the asymptotic value of the non-minimal couplings at early times to be different from zero.

$$\mathbf{EMG} : \left\{ \frac{M^2}{M_{\text{pl}}^2} \rightarrow \text{const.}, \frac{\mu_1}{H} \rightarrow 0, \frac{\mu_2^2}{H^2} \rightarrow \text{const.}, \frac{\mu_3}{H} \rightarrow \text{const.}, \epsilon_4 \rightarrow \text{const.} \right\}_{x \rightarrow 1}. \quad (12)$$

Note that the Brans-Dicke non-minimal coupling μ_1 needs a special attention due to its link with M^2 (see eq. (2)): for any asymptotic value of μ_1 different than zero, M^2 would tend to either zero or plus infinity, corresponding to infinite or zero gravitational coupling respectively. We thus restrict to the cases when $\mu_1 \rightarrow 0$.

The imprints of LDE, EDE and EMG that can be revealed through the analysis of cosmological observables is discussed in Sec. 3.

2.3 Extracting observables

Extracting observables of the perturbation sector in modified gravity (MG) theories is mostly straightforward on cosmic comoving Fourier modes well below the non-linear limit and well above the DE sound horizon. In this regime, linear theory and the *quasi-static approximation* [58, 59] can be trusted. The latter allows one to neglect time derivatives of scalar and metric fluctuations over spatial derivatives. Moreover, in our framework, the extra scalar degree of freedom has the purpose of sourcing cosmic acceleration thus its mass must be of order Hubble or lighter. Therefore, Fourier modes close to the Hubble scale would be the only ones affected by these mass scales. Given that surveys of the LSS observe modes generally deep inside the Hubble horizon, one can thus neglect any scale-dependence in our observables. These observables can be schematically split into two types, the ones linked to the growth of matter perturbations and the ones sensitive to the gravitational potentials. Let us briefly present them, for which we have adopted the following convention for the perturbed metric in Newtonian gauge:

$$ds^2 = -(1 + 2\Phi)dt^2 + a^2(1 - 2\Psi)\delta_{ij}dx^i dx^j. \quad (13)$$

- ◊ **Effective gravitational coupling (μ)**: In most MG theories it is possible to compile a part of the modifications of gravity in an observer-friendly quantity, an effective gravitational coupling μ . It is defined through the Poisson equation, $-\frac{k^2}{a^2}\Phi = 4\pi\mu G_N \rho_m \delta_m$. In [16] it was shown that the Newton constant G_N of an EFT model is defined by:

$$G_N = \frac{1}{8\pi M^2(t_0)[1 + \epsilon_4(x_0)]^2}. \quad (14)$$

The effective gravitational constant in the EFT formulation then yields:

$$\mu = \left(\frac{M(x_0)[1 + \epsilon_4(x_0)]}{M[1 + \epsilon_4]} \right)^2 \frac{a_0}{b_0}, \quad (15)$$

where

$$\begin{aligned} a_0 &= 2\mathcal{C} + \dot{\mu}_3 - 2\dot{H}\epsilon_4 + 2H\dot{\epsilon}_4 + 2(\mu_1 + \dot{\epsilon}_4)^2, \\ b_0 &= 2\mathcal{C} + \dot{\mu}_3 - 2\dot{H}\epsilon_4 + 2H\dot{\epsilon}_4 + 2\frac{(\mu_1 + \dot{\epsilon}_4)(\mu_1 - \mu_3)}{1 + \epsilon_4} - \frac{(\mu_1 - \mu_3)^2}{2(1 + \epsilon_4)^2}, \end{aligned} \quad (16)$$

and

$$\dot{\mu}_3 \equiv \dot{\mu}_3 + \mu_1\mu_3 + H\mu_3, \quad (17)$$

$$\dot{\epsilon}_4 \equiv \dot{\epsilon}_4 + \mu_1\epsilon_4 + H\epsilon_4. \quad (18)$$

- ◇ *Growth function ($f\sigma_8$)*: The effective gravitational constant is naturally part of the source term in the evolution of the linear density perturbations of matter δ :

$$\ddot{\delta} + 2H\dot{\delta} - 4\pi\mu G_N\rho_m\delta = 0. \quad (19)$$

The δ variable is of difficult observability. However its second statistical moment, the *rms* of linear density fluctuations on the characteristic scale $R = 8Mpc/h$, σ_8 , and its logarithmic derivative with respect to the scale factor of the universe, the linear growth rate f , can be combined in an observable quantity ($f\sigma_8$) which is minimally affected by observational biases.²

- ◇ *Gravitational slip parameter (η)*: Gathering modifications of gravity in an effective gravitational constant does not suffice to model all deviations from GR. The Poisson equation must be supplemented with an equation for the gravitational slip parameter, namely the quantity sensitive to differences between the two gravitational potentials, $\eta \equiv \Psi/\Phi$. In the EFT of DE it yields as a function of the couplings:

$$\eta = 1 - \frac{c_0}{a_0}, \quad (20)$$

where

$$c_0 = (\mu_1 + \dot{\epsilon}_4)(\mu_1 + \mu_3 + 2\dot{\epsilon}_4) - \epsilon_4(2\mathcal{C} + \dot{\mu}_3 - 2\dot{H}\epsilon_4 + 2H\dot{\epsilon}_4). \quad (21)$$

Note that μ and η share the same term a_0 . The implication of this constraint will be discussed in Sec. 4.

- ◇ *Light deflection parameter (Σ)*: In general, observations probing the gravitational potentials, such as weak lensing measurements, are not directly sensitive to the gravitational slip parameter but to the or light deflection parameter Σ . In GR, as for η , it is equal to 1. In MG, it is not necessarily and is defined through the equation $-\frac{k^2}{a^2}(\Phi + \Psi) = 8\pi\Sigma(t, k)G_N\rho_m\delta_m$. It can be expressed straightforwardly as a combination of μ and η

$$\Sigma = \frac{\mu}{2}(1 + \eta). \quad (22)$$

This theoretical degeneracy between observables of the perturbed sector will be instrumental in understanding specific predictions of Horndeski theories.

²We predict the amplitude of the present-day value of the *rms* density fluctuations in a given EFT model of gravity, by rescaling the Planck best fitting value $\sigma_8(x_0)$ as follows: $\sigma_8^{EFT}(x) = \frac{D_+^{EFT}(x)}{D_+^{Planck}(x_0)}\sigma_8^{Planck}(x_0)$, where D_+ is the growing mode of linear matter density perturbations.

2.4 Viability criteria

Although asymptotic behaviours of the EFT functions can be changed, not all their possible time scalings are permitted. A healthy theory must indeed fulfil a set of stability conditions: it must not be affected by ghosts, nor by gradient instabilities. Furthermore, along the arguments detailed in [60], we will not allow superluminal propagation speeds for either scalar or tensor modes. On top of these theoretical requirements, we should exclude models that are already ruled out by current observations. As for the choice of the background expansion rate, which we describe via the effective Hubble rate (5), we exploit current limits available in the perturbed sector of the universe. Notably, the local value of gravitational waves of EFT of DE models has been recently constrained leading to a bound on the value of $\epsilon_4(t_0) \sim 10^{-3}$ [61], thus we simply set its present value to 0 for simplicity. In summary,

Stability of the theory,

$$A = (\mathcal{C} + 2\mu_2^2)(1 + \epsilon_4) + \frac{3}{4}(\mu_1 - \mu_3)^2 \geq 0 \quad \text{ghost free,} \quad (23)$$

$$B = b_0 \geq 0 \quad \text{gradient,} \quad (24)$$

Subluminal propagation speeds,

$$c_s^2 = \frac{B}{A} \leq 1 \quad \text{scalar modes,} \quad (25)$$

$$c_T^2 = \frac{1}{1 + \epsilon_4} \leq 1 \quad \text{tensor modes,} \quad (26)$$

Observational requirement (compatibility with current constraints),

$$\epsilon_4(x = x_0) = 0. \quad (27)$$

Since they impose tight constraints on the functional behaviour of relevant observables of the LSS, viability criteria can be effectively used to complement data and observational information in statistical inferences. The dependence of our conclusions on the requirement of sub-luminal propagation speeds will be assessed in Sec. 4.1.

3 General predictions on LSS observables

In this section, we explore the space of theories following the protocol elaborated by [16]: the non-minimal couplings are expanded in power series of $(x - x_0)$ up to order 2 (see Appendix A), where each coefficient is randomly chosen within the window $[-1, 1]$ with a flat uniform prior. This is enough to cover all the rich phenomenology arising in our EFT models. A pre-factor $(1 - x)$ in the expansion is either switched on or off depending on the DE scenario, *i.e* whether a non-minimal coupling needs to vanish at early times or not (see eqs. (10), (11) and (12) for the conditions imposed in the various scenarios). The initial time we consider numerically is set to $z_i = 100$, where radiation is already sub-dominant. It is for example the time where initial conditions are set for the integration of growth observables. We reject the theories that do not pass the viability conditions from early times until today. In addition, to lie within the range of applicability of the quasi-static approximation only models with $c_s^2 > 0.1$ are kept [59]. With this procedure we randomly generate 10^4 viable EFT models of each DE scenario.

For what concerns the class of LDE theories, an important generalization with respect to [16] is that we also consider here the coupling μ_2^2 not to be equal to zero at all times. The latter, although not entering the expressions of the relevant observables, controls the effectiveness of the no-ghost stability condition and thus generally relaxes the selection processes. We then study the implications of early dark energy scenarios (EDE and EMG).

3.1 LDE scenario

A definite feature emerging from inspecting the first row of panels in figure 1, is the peculiar *S-shape* redshift evolution of the effective Newton constant $\mu(z)$ in LDE models. Notably, one has $\mu \geq 1$ at both late ($z \sim 0$) and early epochs ($z > 2$), while power is suppressed in the interval $0.5 < z < 1$, in the sense that in most theories μ is found to be less than 1. This extremely constrained functional behaviour was already noticed by [16] and confirmed by [62], although for a more restricted class of Horndeski models.

The subset of models displaying $\mu > 1$ in the interval $0.5 < z < 1$, despite having small size relative to the entire set of simulated models, has not strictly zero measure as was previously found in [16]. This is the consequence of switching on the non-minimal coupling μ_2^2 which, in the present analysis, it is allowed to vary freely in the interval $[-1, 1]$. Indeed, affecting the sound speed, and more precisely the no-ghost stability condition (23), this parameter induces non-negligible back reactions on the LSS observables. From [16] it was understood that the period of weaker gravity in $\mu(z)$ at intermediate redshifts was induced by the $1/M^2$ component (see eq.(15)). Our current study reveals that switching on μ_2^2 is the necessary condition for LDE models to exhibit $M^2/M_{\text{pl}}^2 < 1$ in a stable way and therefore a subset of theories with $\mu > 1$ at intermediate redshifts, *i.e* stronger gravity and also deeper gravity potentials than the standard model. Since under these conditions light should bend more on average, it does not come as a surprise that models exhibiting $\mu > 1$ in $z \in [0.5, 1]$ also display $\eta > 0$, *i.e* $\Phi > \Psi$, or $\Sigma > 0$, as the inspection of the second and third row of Figure 1 shows.

The bounded evolution history of μ has major implications for the growth of structures, as captured by the $f\sigma_8$ observable. Indeed the effective Newton constant is part of the source term in the equation used to compute the growth factor f :

$$3w_{\text{eff}}(1-x)xf'(x) + f(x)^2 + \left[2 - \frac{3}{2}(w_{\text{eff}}(1-x) + 1)\right]f(x) = \frac{3}{2}x\mu G_{\text{N}}, \quad (28)$$

and also affects the amplitude of σ_8 , the *r.m.s* of the matter density fluctuations. Characteristic features of μ at time x will be seen time translated at later epochs, *i.e* lower x , in the $f\sigma_8$ evolution since the effective source term in eq. (28) is $x\mu$ and since $\sigma_8(z)$ is an integral quantity summed from the past (here $z_i = 100$) until z . Figure 1 shows that amplitude of $f\sigma_8$ expected in a Λ CDM model is always minimal if compared to Horndeski expectations for $z > 1.5$. Interestingly, measurements of low $f\sigma_8$ amplitudes (with respect to the Planck-extrapolated value) provided by local redshift surveys seem to be quasi systematic, especially in analyses where the background is decoupled from the perturbation sector, see for instance [63–66]. In parallel, recent observations at higher redshifts $z \sim 1.4$ [67], seem to be suggestive of an early epoch with an excess of growth with respect to standard model predictions, although the error bar being too large does not yet allow to draw any meaningful interpretations. However, it serves as an illustration that, if such values were to hold up, they would effectively confirm a definitive prediction of Horndeski theories.

The remarkable tightness of the growth rate evolution of $f\sigma_8(z)$ also deserves a comment. Despite μ , η and Σ spanning, especially at low redshift, a large range of values, absolute deviations of $f\sigma_8$ from the Λ CDM prediction are never larger than 0.2 at all cosmic epochs investigated. The remarkably low theoretical dispersion, or equivalently, the poor sensitivity of $f\sigma_8$ to the variation of the Horndeski couplings, is not however prejudicial, from the observational side, for the purposes of model identification. Indeed, it is as well remarkable that no single model displays both $f\sigma_8 < 0$ and $\Sigma > 0$ for any $z > 1$. Measurements of $f\sigma_8$ from redshift surveys, when combined with lensing estimations of Σ , provide thus an interesting diagnostic tool: evidences of even a single data point lying in the top right quadrant of the $f\sigma_8 - \Sigma$ plane at

redshift larger than 1 would definitely rule out LDE of the Horndeski type as a viable candidate for theoretical interpretation.

Among the features emerging from Figure 1 is a strong positive correlation between μ and Σ at high redshifts, or, even more telling, the lack of theories predicting $\mu - 1$ and $\Sigma - 1$ of opposite sign as long as $z > 0.5$. When the behaviour of the gravitational slip parameter is closely scrutinized, the fact that η and μ cannot be both positive once $z > 1$ also stands out.

The question is now whether any violation of these features is a smoking gun of the failure of only the LDE models, or, more interestingly, if it can rule out even more general Horndeski scenarios. This issue is investigated in the next section.

LDE :

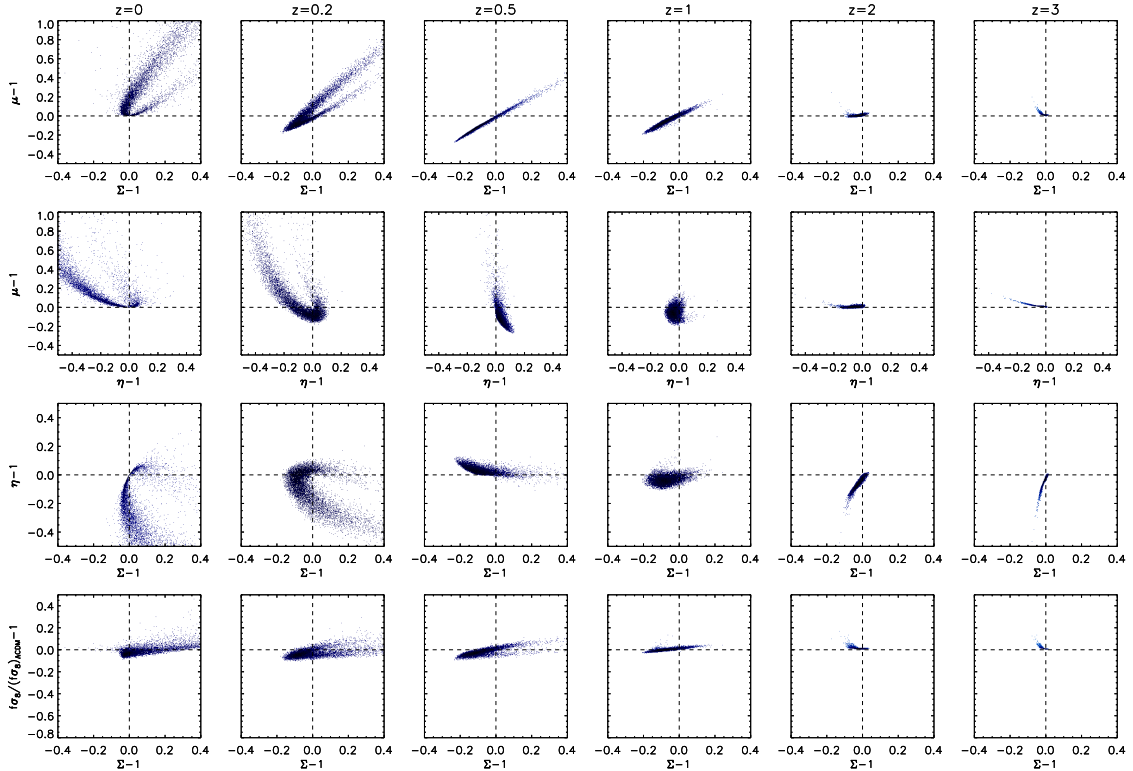


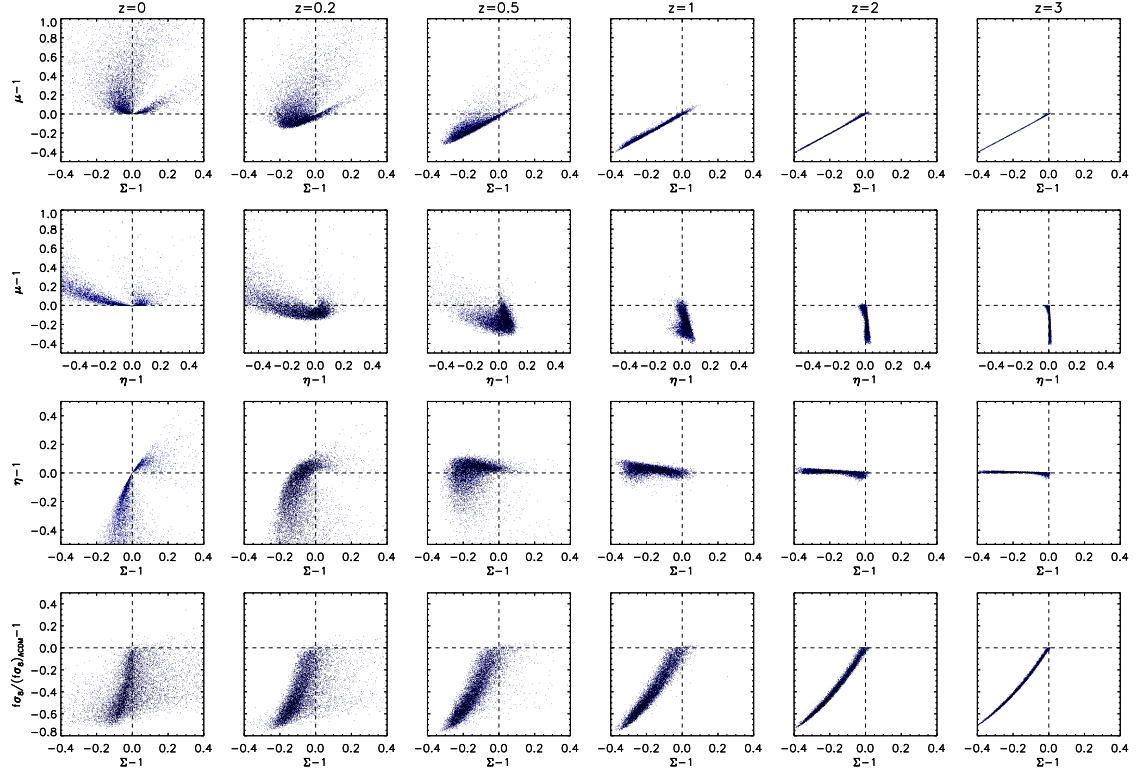
Figure 1: The correlations between μ , η , Σ and $f\sigma_8$ is displayed at several redshift epochs, from left to right $z = 0, 0.2, 0.5, 1, 2, 3$, for 10^4 EFT models in the LDE scenario. The background evolution has been set to match that of a flat Λ CDM model. The Λ CDM prediction corresponds to the intersection of the two dashed lines. The gray scale highlights the density of points.

3.2 EDE and EMG scenarios

The classification scheme proposed in Sec. 2.2 contains the possibility that dark energy is present at early times, either in the energy momentum tensor (EDE) or also as early modified gravity (EMG). Figure 2 shows that the presence of modifications of GR at early times alters the values of LSS observables even in the local universe.

Irrespectively of the specific scenario, viability conditions favour theories with μ smaller than 1 for $z > 0.5$. Despite we are now allowing initial values of M^2 different than M_{pl}^2 , the tendency of having $M^2 > M_{\text{pl}}^2$ is surviving. On the other hand, the EMG scenario is the only possibility to produce a small subset of models with $\mu > 1$ at early times.

EDE :



EMG :

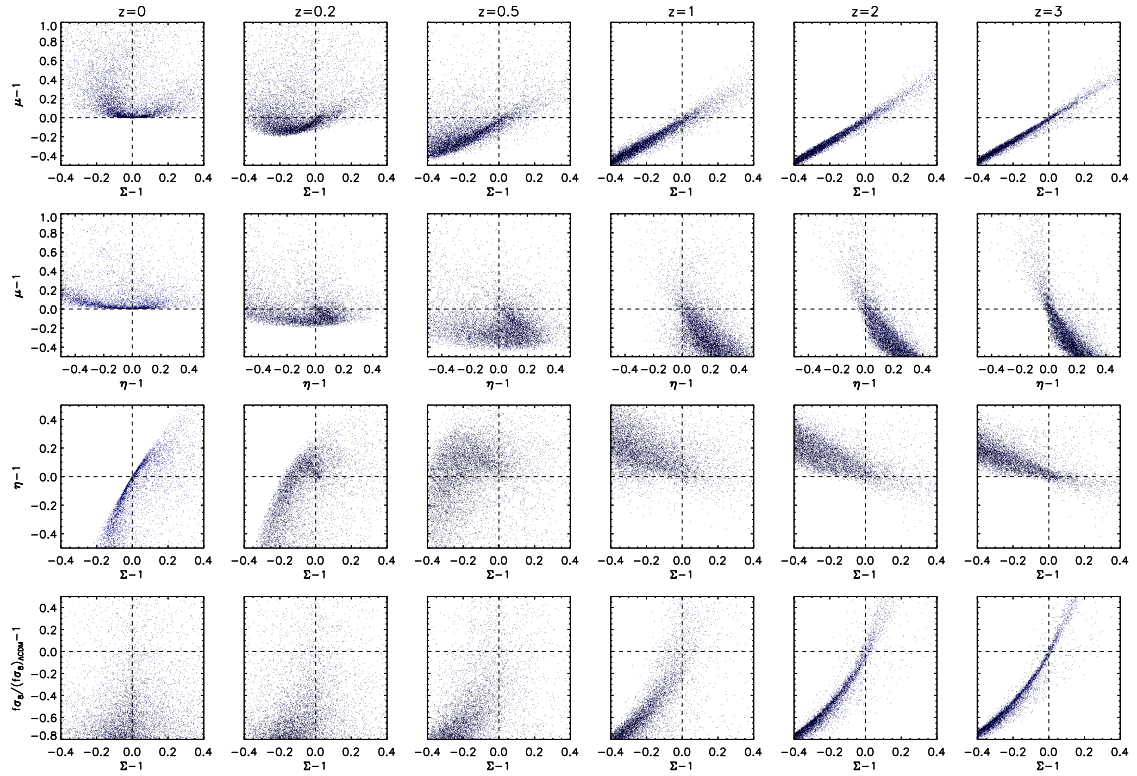


Figure 2: Same as in figure 1 but for 10^4 models in the EDE scenario (top 4 rows) and for 10^4 models in the EMG scenario (bottom 4 rows).

This can be understood by expressing the effective gravitational constant as

$$\mu = \frac{M^2(t_0)[1 + \epsilon_4(t_0)]^2}{M^2(1 + \epsilon_4)^2} \left[1 + \frac{1 + \epsilon_4}{B} \left(\frac{\mu_1 - \mu_3}{1 + \epsilon_4} - (\mu_1 + \epsilon_4) \right)^2 \right]. \quad (29)$$

From stability requirements, $B \geq 0$ and $\epsilon_4 \geq -1$ ($c_T \geq 0$), *i.e.* respectively no gradient instabilities of scalar and tensor modes, the quantity contained in the squared brackets above is greater than or equal to 1. Therefore, allowing non vanishing ϵ_4 and μ_3 at $x = 1$ pushes up the value of μ at early times. The above expression also shows that the value of μ at the present time, $\mu(t_0)$, is always greater than or equal to 1 whatever the DE scenario.

The behaviour of μ at early times affects the $f\sigma_8$ observable at late epochs. For instance, the amplitude of $f\sigma_8$ predicted in EDE scenarios is lower than the standard Λ CDM value for $z > 0.5$, as opposed to LDE, for which models systematically flip over Λ CDM at $z \gtrsim 1.5$. Therefore, over almost all the most interesting epochs of the universe, the Λ CDM growth history appears as an extremum not only among the whole class of LDE models, but also when EDE scenarios are considered. Intriguingly, only EDE models manage to strongly suppress the amplitude of the linear growth function at present time. On the opposite, the only models allowing for a faster growth than Λ CDM (with $f\sigma_8$ more than 20% higher), are the EMG scenarios. This is not surprising for, as we said, it is the only set-up for which $\mu > 1$ at early times.

The asymptotic value of the gravitational slip parameter η at $x = 1$ is, by definition, 1 when the coupling functions μ_3 and ϵ_4 vanish. Therefore, only very mild differences arise between LDE and EDE at early times. On the contrary, the redshift dependence of η is significantly affected in the EMG case, since μ_3 and ϵ_4 are different from zero at all cosmic epochs. As far as the evolution of Σ is concerned, the amplitude calculated in LDE and EDE scenarios is always lower than Λ CDM for $z > 1.5$. Once more, the standard model appears as an extremal model.

EMG is the only mechanism to allow $\Sigma > 1$ also at high redshifts. The marked positive correlation between μ and Σ for $z > 1.5$ persists in EDE models. In fact, since

$$\mu - 1 = \left(\frac{2}{1 + \eta} \right) (\Sigma - 1) - \frac{\eta - 1}{1 + \eta}, \quad (30)$$

a clear 45° correlation should be seen as long as η is close to unity. This is well seen in the cases for LDE and EDE scenarios at high redshifts as opposed to the EMG scenario which displays slightly more dispersion, for it exhibits larger η .

Assuming a non-standard gravitational signal will be detected by future surveys, we can thus tentatively conclude from comparing Figs. 1 and 2 that the Horndeski class of models will definitely be ruled out as a modified gravity candidate if μ and Σ have different sign for $z > 1.5$. The same conclusion holds if future estimates should eventually converge on a local ($z = 0$) value of the effective Newton constant lower than 1.

We stress that finding $\mu - 1$ and $\Sigma - 1$ of opposite signs at any redshift would not rule out all Horndeski models. For instance, the fact that η displays the larger set of values around present time, the relation (30) induces the models to spread on either side of the $\mu = 1$ line and $\Sigma > 1$ in the μ - Σ plane. As a matter of fact, in the EMG case for $z = 0$ we observe a ratio of $\approx 53\%$ models on the left quadrant and $\approx 47\%$ on the right. Nevertheless, a clear correlation between μ and Σ in various interesting higher redshift intervals is definitely confirmed by our analysis (see also figure 6 in [16]). Therefore, we find that the μ - Σ plane can be used as a discriminant only in a limited redshift range ($z \gtrsim 1.5$) and upon imposing our viability conditions. We refer to Figure 4 below to display how the “opposite signs” statement is progressively weakened by the relaxation of some of our conditions. These aspects are also highlighted in Figure 7 of [68], where CMB data likelihood is plotted for the observables μ and Σ calculated at $z = 0$.

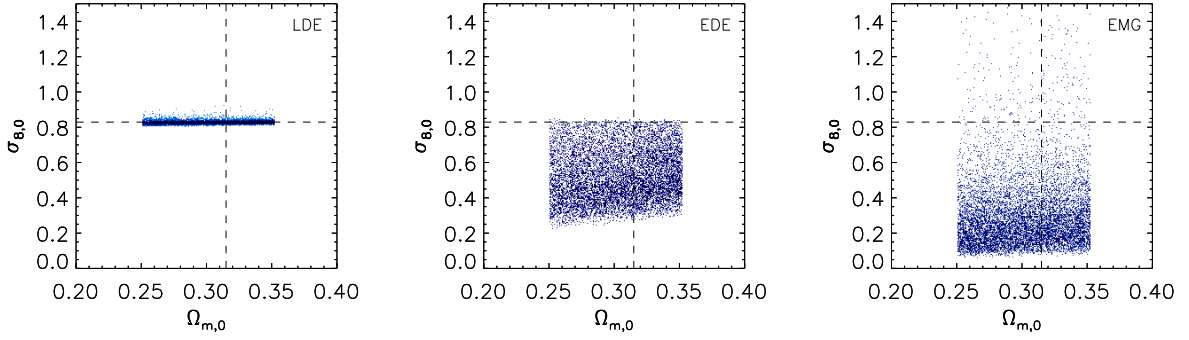


Figure 3: Present day value of σ_8 as a function of the fractional matter density today $\Omega_{m,0}$ of 10^4 EFT models. Here, the value of $\Omega_{m,0}$ per model is left as free parameter and is randomly generated, as are the coefficients of the coupling functions. The background has been set to a flat Λ CDM background. The intersection of the dashed lines corresponds to the Planck measurements [39].

In much the same way as the plane μ – Σ provides a diagnostic for the whole class of Horndeski models, the plane $f\sigma_8$ – Σ allows us to tell apart Horndeski dark energy sub-classes. For example, if $f\sigma_8 > (f\sigma_8)_{\Lambda\text{CDM}}$ at $z > 1.5$, then EDE scenarios are ruled out. Similarly, LDE is not viable if both $f\sigma_8$ and Σ have smaller amplitude than predicted by Λ CDM for $z > 1.5$.

Identical conclusions follow from the analysis of the amplitude of the σ_8 observable alone. Figure 3 shows the present-day linear extrapolation of the *rms* fluctuations of the matter density field, which we assume to be normalized by the Planck measurements at last scattering. Predictions closely reproduce the Λ CDM limit in all the LDE models. However, a local measurement of σ_8 showing large deviations from the Λ CDM extrapolation will be instrumental for disentangling EDE from EMG scenarios. The first would be definitely ruled out if observational evidences should indicate that $\sigma_{8,0} \gtrsim 0.9$.³

In summary, we find the effects of early modification of GR to be conspicuous also at low redshift. Joint measurements of the η , Σ and $f\sigma_8$ observables would give strong indications as to the type of DE required for a faithful description of cosmological perturbations. Indeed, complementing an analysis on the growth of structures with lensing observables increases substantially the discriminating power between models.

4 Discussion

The next issue we tackle concerns the generality and robustness of our findings against changes in the specific settings and/or assumptions adopted in the analysis. We first explore whether our diagnostic predictions still stand out so clearly once some viability conditions about propagations speeds are relaxed. Then, we gauge the effects of considering non-standard evolution of the background expansion rate. Finally, we discuss additional checks on the generality of our results and the parametrisation of Horndeski theories.

³We note that lower values of σ_8 are also found in the “kinetic matter mixing” model considered in [56].

4.1 Constraining power of viability conditions

When dealing with the dark sector it is still debated if super-luminal propagation in a low-energy effective theory can be acceptable. We tend to see super-luminality as a serious pathology of a low-energy theory, following the reasoning in [60]. However, for the sake of generality, in Figure 4 we show the effects of relaxing the conditions on the propagation speeds of the scalar and the tensors, eqs. (25) and (26). We never intend to give up either ghost stability (23) nor gradient stability (24)—gathered henceforth under the notation S . It is worth noting that, in our formalism, a theory exhibiting $c_s > 1$ can always be tuned back to $c_s \leq 1$ by using the parameter μ_2^2 . The latter, we recall, does not enter the expressions of the LSS observables. Therefore, switching on μ_2^2 allows one to include Horndeski models with $c_s > 1$ but $\mu_2^2 = 0$, in some sense. This is, in Figure 4, implementing the conditions S and the condition $S + c_s$ produces plots. One can rightfully conclude that the selection criterion $c_s < 1$ is useless once a non null μ_2^2 is considered.

On the other hand, by writing μ as $\mu = \left(\frac{c_T}{c_T(t_0)}\right)^4 \frac{M^2(t_0)}{M^2} \frac{a_0}{b_0}$ one already appreciates analytically how $c_T > 1$ strengthens gravity at high redshifts. This is well highlighted by Figure 4, the correlation lines of in the μ - Σ or $f\sigma_8$ - Σ planes are thinner once the $c_T \leq 1$ is implemented, the upper points being chopped out. The practical conclusion out of this analysis is if a data point was to be found at high redshifts in the top left corner of either the μ - Σ or $f\sigma_8$ - Σ plane, only a Horndeski model with a $c_T > 1$ would be valid. More will be able to be said once c_T is tightly constrained at large redshifts by future measurements of the electromagnetic counter part of gravitational wave emitting events [69].

4.2 Effects of the background expansion history

Does the evolution of perturbed sector observables depend on the acceleration of the background metric?

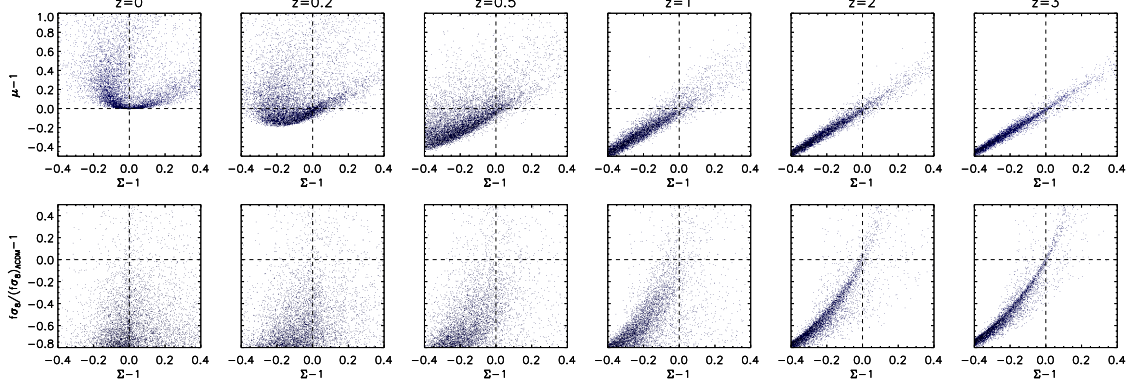
What we find is that setting $w_{\text{eff}} = -0.9$ does not change the diagnostic described in the previous section—we do not display any plot for the sake of brevity.

The effect of lowering the dark energy equation of state below $w_{\text{eff}} = -1$ is also very mild, but worth commenting. Crossing the $w_{\text{eff}} = -1$ means considering violations of the null energy condition. As known, such violation can be produced in a stable theory only by switching on the non-minimal gravitational couplings (see Figs. 1 and 2 of Ref. [15]), and therefore in a region of the space of theories that is “far” from Λ CDM where all couplings vanish. Nevertheless, the effects of modified gravity are not significantly amplified as can be seen by the comparison between Figure 5 and Figs. 1 and Figure 2 (lower panel). The amplification effect is effectively compensated by the wide variations of the couplings and by the large volume in the theory space that we are considering, even in the $w_{\text{eff}} = -1$ case. In summary, we do not find distinctive definite features of LSS phenomenology related to stable violations of the null energy condition.

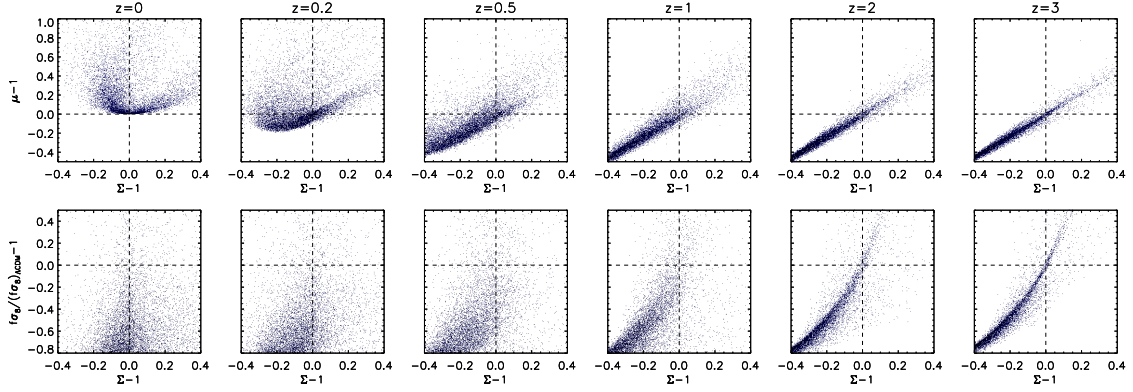
4.3 Consistency and robustness checks

To assess the generality of our results we have conducted two consistency checks. From the analysis undertaken in this paper and in [15, 16, 68], the Λ CDM paradigm stands out as an extremal model among EFT models. However, one could wonder whether our randomly generated coefficients within a uniform distribution could end up favouring models that are very far from the standard paradigm. However, we have checked that the correlations we find are unchanged even if the coefficients are picked from Gaussian distributions centred around 0 (the Λ CDM value) and with a standard deviation of 1.

S :



$S + c_s$:



$S + c_T$:

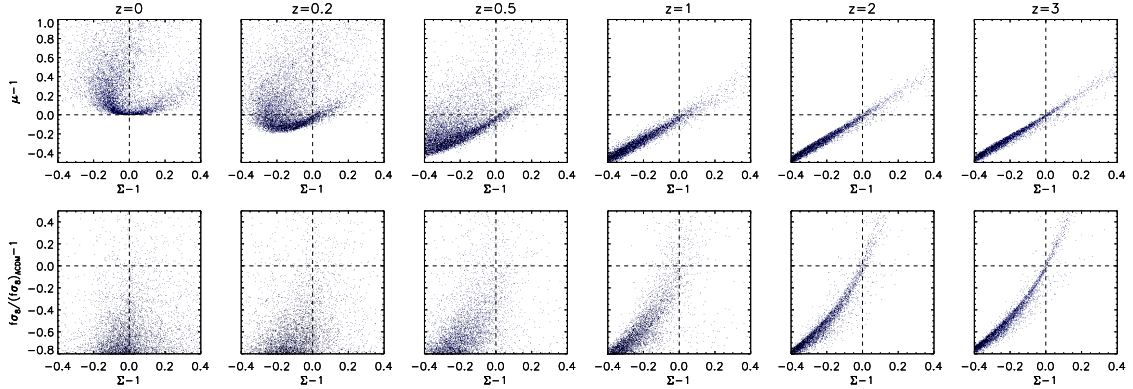
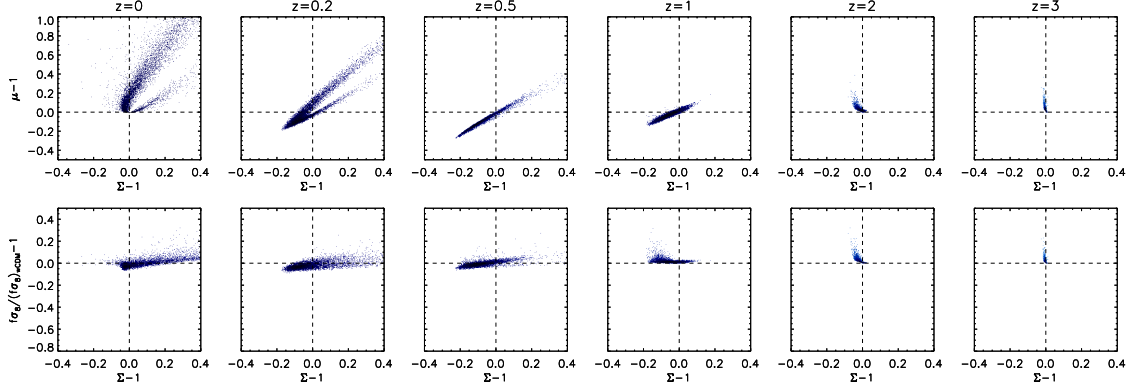


Figure 4: Correlations in the μ - Σ and $f\sigma_8$ - Σ planes for 10^4 EMG models with the stability condition S (first two rows), the stability condition S and $c_s \leq 1$ (middle two rows) and the stability condition S and $c_T \leq 1$ (bottom two rows). The background evolution has been set to a flat Λ CDM. The Λ CDM prediction stands at the intersection of the two dashed lines.

LDE :



EMG :

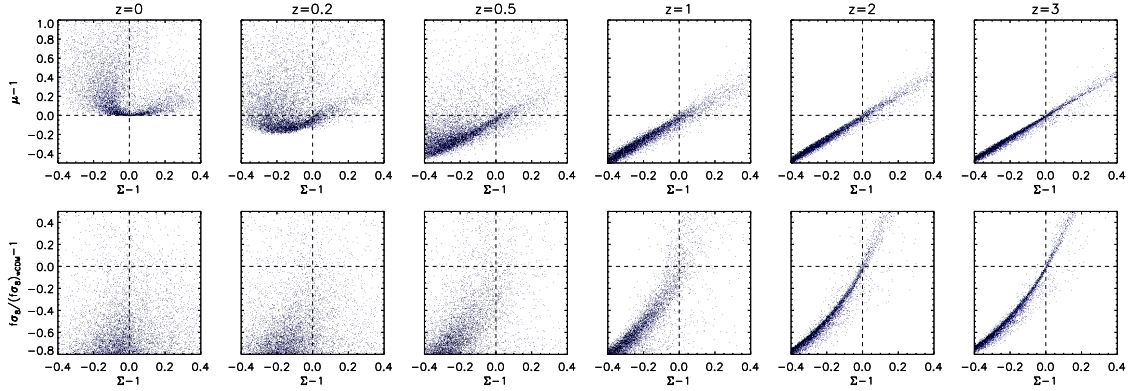


Figure 5: Correlations in the μ - Σ and $f\sigma_8$ - Σ for 10^4 LDE models (two top rows) and 10^4 EMG models (bottom two rows) with the full viability conditions requested but the background *e.o.s* set to $w_{\text{eff}} = -1.1$. The $(w = -1.1)\text{CDM}$ prediction corresponds to the crossing of the two dashed lines.

As a second check, we have noted that our diagnostic is also unchanged under using a different parametrisations of the couplings. In particular we have considered an alternative choice of the coupling functions, the so called " α -parametrisation" first proposed by [70] and extended by [53–55, 71, 72], as opposed to the " μ -parametrisation" presented in this paper. Appendix B contains a dictionary to switch between the two parametrisations.

5 Conclusions

What Horndeski theories have to say about early dark energy? This is the original question motivating the analysis presented in this paper. Early modifications of GR are found to have non-negligible, lasting and potentially detectable effects in the LSS observables of the local and recent universe.

In Figure 6 we summarize our main findings. By tracing the time evolution, from early epochs ($z = 100$) down to present day, of fundamental LSS observables such as the reduced effective Newton constant μ , the gravitational slip parameter η , the lensing parameter Σ and the linear growth function of LSS $f\sigma_8$ we have found that GR extensions contemplating an additional scalar degree of freedom with second order equations of motion can be definitely ruled out if one of the following conditions apply (Figure 6, left panel):

- The observables μ and Σ have opposite sign for $z > 1.5$
- $\mu < 1$ at $z = 0$

Specific sub-classes of such theories in which the modified gravity effects are limited to late times could be discriminated if data at redshift $z > 1.5$ eventually become available for both redshift and lensing surveys. Indeed, we find that above that critical redshift

- LDE will be ruled out if $f\sigma_8 < (f\sigma_8)_{\Lambda CDM}$ at $z > 1.5$
- EDE will be ruled out if $f\sigma_8 > (f\sigma_8)_{\Lambda CDM}$ at $z > 1.5$ or $f\sigma_8 > (f\sigma_8)_{\Lambda CDM}$ and $\Sigma > 1$ at $z > 1.5$

These results are insensitive to the background dark energy *e.o.s* parameter within the reasonable range $w_{\text{eff}} \in [-1.1, -0.9]$. Indeed, we have found the diagnostic tool does not lose predictability when progressively less constraining requirements are imposed.

Two complementary strategies allow to estimate the likelihood of data given the Horndeski class of theories. A model-dependent analysis is optimal if one is to exploit theoretical priors about the physical viability of specific Horndeski models to complement the discriminatory power of data. Indeed, [68] have shown that by this approach the region of the parameter space that is not rejected by observations is significantly reduced. An orthogonal approach consists in implementing model-independent likelihood analysis, parametrising LSS observables in a purely phenomenological way, blindly of any gravitational theory. The diagnostics developed in this paper are meant to facilitate theoretical interpretation in these cases. Interestingly, model-independent analyses have been pursued for example in [12] and more recently in [73] and preliminary results are suggestive of a negative value of $\mu - 1$ at redshift $z = 0$. Should future, higher precision data strengthen the statistical significance of these findings, the Horndeski landscape would face hard times.

Exploring beyond standard GR, and notably the functional space of scalar-field extension of GR will eventually become less disorienting than previously suspected. However, much must still be accomplished and a number of improvements would be desirable. We have focused on

scales much smaller than the Hubble radius in this paper. As data improve on ever larger scales, our analysis should be extended to include possible scale dependent effects coming from mass terms of the scalar field that are of the order of Hubble. Lastly, it would be useful to study to which level our diagnostic plots are stable to the inclusions of more general scenarios in which the scalar field is allowed to satisfy larger than second order equation of motions (the so called beyond Horndeski theories [52, 74])

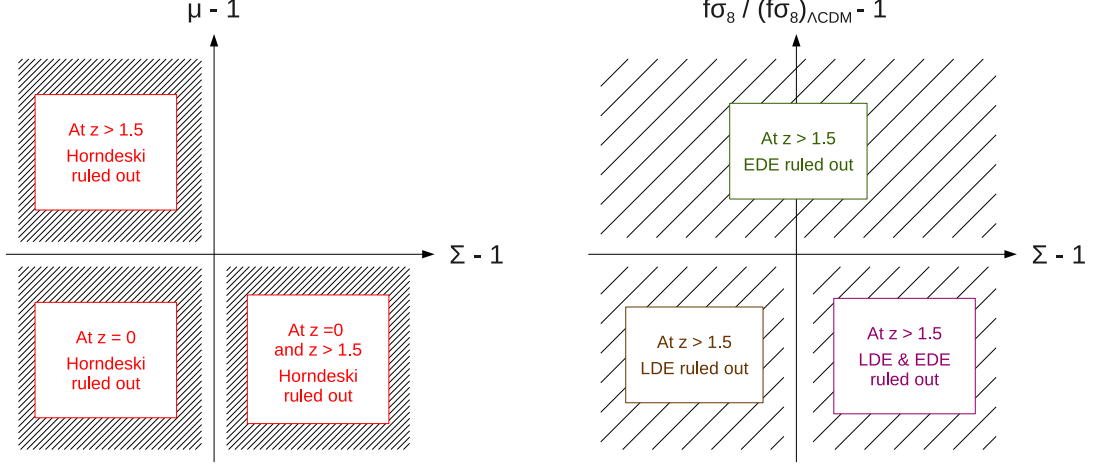


Figure 6: Schematics of the fundamental observable planes allowing to discard Horndeski theories (left diagram) and the type of dark energy embedded (right diagram).

Acknowledgments

We acknowledge useful discussions with Jose Beltràn Jiménez, Julien Bel, Lam Hui, Stephane Ilić, Levon Pogorian, Valentina Salvatelli, Alessandra Silvestri and Filippo Vernizzi. F.P. warmly acknowledges the financial support of A*MIDEX project (n° ANR-11-IDEX-0001-02) funded by the “Investissements d’Avenir” French Government program, managed by the French National Research Agency (ANR). CM is grateful for support from specific project funding of the Labex OCEVU. This article is based upon work from COST Action CANTATA CA15117, supported by COST (European Cooperation in Science and Technology).

A Parametrisation of the couplings

In this appendix we present how we parametrise the EFT coupling functions in the three different DE scenarios.

LDE and EDE :

$$\mu(x) = H (1 - x) \left(p_{11} + p_{12} (x - \Omega_{m,0}) + p_{13} (x - \Omega_{m,0})^2 \right), \quad (31)$$

$$\mu_2^2(x) = H^2 (1 - x) \left(p_{21} + p_{22} (x - \Omega_{m,0}) + p_{23} (x - \Omega_{m,0})^2 \right), \quad (32)$$

$$\mu_3(x) = H (1 - x) \left(p_{31} + p_{32} (x - \Omega_{m,0}) + p_{33} (x - \Omega_{m,0})^2 \right), \quad (33)$$

$$\epsilon_4(x) = (1 - x) \left(p_{42} (x - \Omega_{m,0}) + p_{43} (x - \Omega_{m,0})^2 \right). \quad (34)$$

For the LDE case the constrain $p_{12} = \frac{p_{11} \log(\Omega_m^0) - 6 \log(1 + (1 - \Omega_m^0) p_{41})}{1 - \Omega_m^0 + \Omega_m^0 \log(\Omega_m^0)}$ must be imposed to enforce $M^2(x \rightarrow 1) \rightarrow M_{\text{pl}}^2$, see [16] for details.

EMG :

$$\mu(x) = H (1 - x) \left(p_{11} + p_{12} (x - \Omega_{m,0}) + p_{13} (x - \Omega_{m,0})^2 \right), \quad (35)$$

$$\mu_2^2(x) = H^2 \left(p_{21} + p_{22} (x - \Omega_{m,0}) + p_{23} (x - \Omega_{m,0})^2 \right), \quad (36)$$

$$\mu_3(x) = H \left(p_{31} + p_{32} (x - \Omega_{m,0}) + p_{33} (x - \Omega_{m,0})^2 \right), \quad (37)$$

$$\epsilon_4(x) = \left(p_{42} (x - \Omega_{m,0}) + p_{43} (x - \Omega_{m,0})^2 \right). \quad (38)$$

B Links with the α -parametrisation

The EFT action of Horndeski theories for linear perturbations about an FLRW background can be also parametrised by

$$S = \int d^3x dt a^3 \frac{M_*^2}{2} \left[\delta K_{ij} \delta K^{ij} - \delta K^2 + {}^{(3)}R \delta N \right. \\ \left. + (1 + \alpha_T) \left({}^{(3)}R \frac{\delta \sqrt{h}}{a^3} \right) + \alpha_K H^2 \delta N^2 + 4\alpha_B H \delta K \delta N \right], \quad (39)$$

with N being the lapse function and S_m the action of matter perturbations in the Jordan frame.

In this action the EFT couplings stand as a running planck mass M_* , the excess speed of gravitational waves, the kineticity α_K and the braiding α_M . It customary to redefine the running of the planck mass trough the non minimal coupling $\alpha_M = \frac{1}{H} \frac{d \ln M_*^2}{d \ln t}$. The alpha parametrisation has the benefit of attaching the evolution coupling functions to clear physical effects. However, the theory-friendly view point is lost, subsets of Horndeski theories, such as Brans-Dicke for instance, are described by more involved combinations of the α functions as compared to the μ 's (see table 1 in [15]). In parallel, the μ -parametrisation has the benefit of displaying a Lagrangian expanded in small perturbations where the couplings are expected to be of order 1.

The mapping with the μ -characterisation is the following.

$$M_* = M \sqrt{1 + \epsilon_4} \quad (40)$$

$$\alpha_M = \frac{\dot{\epsilon}_4}{H(1 + \epsilon_4)} + \frac{\mu_1}{H} \quad (41)$$

$$\alpha_K = \frac{2\mathcal{C} + 4\mu_2^2}{H^2(1 + \epsilon_4)} \quad (42)$$

$$\alpha_B = \frac{\mu_1 - \mu_3}{2H(1 + \epsilon_4)} \quad (43)$$

$$\alpha_T = -\frac{\epsilon_4}{1 + \epsilon_4} \quad (44)$$

$$(45)$$

From this, the DE scenarios are characterised by:

$$\begin{aligned}
\mathbf{LDE} &: \left\{ \frac{M_*^2}{M_{\text{pl}}^2} \rightarrow 1, \alpha_M \rightarrow 0, \alpha_K \rightarrow 0, \alpha_B \rightarrow 0, \alpha_T \rightarrow 0 \right\}_{x \rightarrow 1}, \\
\mathbf{EDE} &: \left\{ \frac{M_*^2}{M_{\text{pl}}^2} \rightarrow \text{const.}, \alpha_M \rightarrow 0, \alpha_K \rightarrow \text{const.}, \alpha_B \rightarrow 0, \alpha_T \rightarrow 0 \right\}_{x \rightarrow 1}, \\
\mathbf{EMG} &: \left\{ \frac{M_*^2}{M_{\text{pl}}^2} \rightarrow \text{const.}, \alpha_M \rightarrow 0, \alpha_K \rightarrow \text{const.}, \alpha_B \rightarrow \text{const.}, \alpha_T \rightarrow \text{const.} \right\}_{x \rightarrow 1}.
\end{aligned}$$

References

- [1] <http://www.darkenergysurvey.org>.
- [2] <http://www.euclid-ec.org>.
- [3] L. Amendola et al., *Cosmology and Fundamental Physics with the Euclid Satellite*, [arXiv:1606.0018](#).
- [4] L. Taddei, M. Martinelli, and L. Amendola, *Model-independent constraints on modified gravity from current data and from the Euclid and SKA future surveys*, [arXiv:1604.0105](#).
- [5] <http://desi.lbl.gov/cdr/>.
- [6] <http://www.lsst.org/lsst/>.
- [7] <http://wfirst.gsfc.nasa.gov>.
- [8] <http://www.skatelescope.org>.
- [9] P. Bull, *Extending cosmological tests of General Relativity with the Square Kilometre Array*, *Astrophys. J.* **817** (2016), no. 1 26, [[arXiv:1509.0756](#)].
- [10] S. Camera et al., *Cosmology on the Largest Scales with the SKA*, *PoS AASKA14* (2015) 025.
- [11] L. Pogosian, A. Silvestri, K. Koyama, and G.-B. Zhao, *How to optimally parametrize deviations from General Relativity in the evolution of cosmological perturbations?*, *Phys. Rev.* **D81** (2010) 104023, [[arXiv:1002.2382](#)].
- [12] F. Simpson et al., *CFHTLenS: Testing the Laws of Gravity with Tomographic Weak Lensing and Redshift Space Distortions*, *Mon. Not. Roy. Astron. Soc.* **429** (2013) 2249, [[arXiv:1212.3339](#)].
- [13] G. W. Horndeski, *Second-order scalar-tensor field equations in a four-dimensional space*, *Int. J. Theor. Phys.* **10** (1974) 363–384.
- [14] C. Deffayet, S. Deser, and G. Esposito-Farese, *Generalized Galileons: All scalar models whose curved background extensions maintain second-order field equations and stress-tensors*, *Phys. Rev.* **D80** (2009) 064015, [[arXiv:0906.1967](#)].
- [15] F. Piazza, H. Steigerwald, and C. Marinoni, *Phenomenology of dark energy: exploring the space of theories with future redshift surveys*, *JCAP* **1405** (2014) 043, [[arXiv:1312.6111](#)].
- [16] L. Perenon, F. Piazza, C. Marinoni, and L. Hui, *Phenomenology of dark energy: general features of large-scale perturbations*, *JCAP* **1511** (2015), no. 11 029, [[arXiv:1506.0304](#)].
- [17] L. Perenon, *General features of single-scalar field dark energy models*, 2016. [arXiv:1607.0691](#).
- [18] L. Pogosian and A. Silvestri, *What can Cosmology tell us about Gravity? Constraining Horndeski with Sigma and Mu*, [arXiv:1606.0533](#).
- [19] C. Wetterich, *Cosmology and the Fate of Dilatation Symmetry*, *Nucl. Phys.* **B302** (1988) 668.

- [20] B. Ratra and P. J. E. Peebles, *Cosmological Consequences of a Rolling Homogeneous Scalar Field*, *Phys. Rev.* **D37** (1988) 3406.
- [21] R. R. Caldwell, R. Dave, and P. J. Steinhardt, *Cosmological imprint of an energy component with general equation of state*, *Phys. Rev. Lett.* **80** (1998) 1582–1585, [[astro-ph/9708069](#)].
- [22] A. Hebecker and C. Wetterich, *Natural quintessence?*, *Phys. Lett.* **B497** (2001) 281–288, [[hep-ph/0008205](#)].
- [23] M. Doran, J.-M. Schwindt, and C. Wetterich, *Structure formation and the time dependence of quintessence*, *Phys. Rev.* **D64** (2001) 123520, [[astro-ph/0107525](#)].
- [24] C. Wetterich, *Quintessence: The Dark energy in the universe?*, *Space Sci. Rev.* **100** (2002) 195–206, [[astro-ph/0110211](#)].
- [25] R. Bean, S. H. Hansen, and A. Melchiorri, *Early universe constraints on a primordial scaling field*, *Phys. Rev.* **D64** (2001) 103508, [[astro-ph/0104162](#)].
- [26] C. Wetterich, *Phenomenological parameterization of quintessence*, *Phys. Lett.* **B594** (2004) 17–22, [[astro-ph/0403289](#)].
- [27] M. Doran and G. Robbers, *Early dark energy cosmologies*, *JCAP* **0606** (2006) 026, [[astro-ph/0601544](#)].
- [28] E. Calabrese, D. Huterer, E. V. Linder, A. Melchiorri, and L. Pagano, *Limits on dark radiation, early dark energy, and relativistic degrees of freedom*, *Phys. Rev. D* **83** (Jun, 2011) 123504.
- [29] C. L. Reichardt, R. de Putter, O. Zahn, and Z. Hou, *New limits on Early Dark Energy from the South Pole Telescope*, *Astrophys. J.* **749** (2012) L9, [[arXiv:1110.5328](#)].
- [30] S. Tsujikawa, *Quintessence: A Review*, *Class. Quant. Grav.* **30** (2013) 214003, [[arXiv:1304.1961](#)].
- [31] **Atacama Cosmology Telescope** Collaboration, J. L. Sievers et al., *The Atacama Cosmology Telescope: Cosmological parameters from three seasons of data*, *JCAP* **1310** (2013) 060, [[arXiv:1301.0824](#)].
- [32] M. Archidiacono, L. Lopez-Honorez, and O. Mena, *Current constraints on early and stressed dark energy models and future 21 cm perspectives*, *Phys. Rev.* **D90** (2014), no. 12 123016, [[arXiv:1409.1802](#)].
- [33] V. Pettorino, L. Amendola, and C. Wetterich, *How early is early dark energy?*, *Phys. Rev.* **D87** (2013) 083009, [[arXiv:1301.5279](#)].
- [34] D. Shi and C. M. Baugh, *Can we distinguish early dark energy from a cosmological constant?*, [arXiv:1511.0069](#).
- [35] B.-Y. Pu, X.-D. Xu, B. Wang, and E. Abdalla, *Early dark energy and its interaction with dark matter*, *Phys. Rev.* **D92** (2015), no. 12 123537, [[arXiv:1412.4091](#)].
- [36] P. Brax, C. van de Bruck, S. Clesse, A.-C. Davis, and G. Sculthorpe, *Early Modified Gravity: Implications for Cosmology*, *Phys. Rev.* **D89** (2014), no. 12 123507, [[arXiv:1312.3361](#)].
- [37] N. A. Lima, V. Smer-Barreto, and L. Lombriser, *Constraints on decaying early modified gravity from cosmological observations*, [arXiv:1603.0523](#).
- [38] **SDSS** Collaboration, M. Betoule et al., *Improved cosmological constraints from a joint analysis of the SDSS-II and SNLS supernova samples*, *Astron. Astrophys.* **568** (2014) A22, [[arXiv:1401.4064](#)].
- [39] **Planck** Collaboration, P. A. R. Ade et al., *Planck 2015 results. XIII. Cosmological parameters*, [arXiv:1502.0158](#).
- [40] E. Aubourg, et al., *Cosmological implications of baryon acoustic oscillation measurements*, *Phys. Rev.* **D92** (2015), no. 12 123516, [[arXiv:1411.1074](#)].
- [41] P. Creminelli, G. D’Amico, J. Norena, and F. Vernizzi, *The Effective Theory of Quintessence: the w_j-1 Side Unveiled*, *JCAP* **0902** (2009) 018, [[arXiv:0811.0827](#)].

- [42] G. Gubitosi, F. Piazza, and F. Vernizzi, *The Effective Field Theory of Dark Energy*, *JCAP* **1302** (2013) 032, [[arXiv:1210.0201](#)]. [[JCAP1302,032\(2013\)](#)].
- [43] J. Gleyzes, D. Langlois, F. Piazza, and F. Vernizzi, *Essential Building Blocks of Dark Energy*, *JCAP* **1308** (2013) 025, [[arXiv:1304.4840](#)].
- [44] J. K. Bloomfield, E. E. Flanagan, M. Park, and S. Watson, *Dark energy or modified gravity? An effective field theory approach*, *JCAP* **1308** (2013) 010, [[arXiv:1211.7054](#)].
- [45] J. Bloomfield, *A Simplified Approach to General Scalar-Tensor Theories*, *JCAP* **1312** (2013) 044, [[arXiv:1304.6712](#)].
- [46] F. Piazza and F. Vernizzi, *Effective Field Theory of Cosmological Perturbations*, *Class. Quant. Grav.* **30** (2013) 214007, [[arXiv:1307.4350](#)].
- [47] L. A. Gergely and S. Tsujikawa, *Effective field theory of modified gravity with two scalar fields: dark energy and dark matter*, *Phys. Rev.* **D89** (2014), no. 6 064059, [[arXiv:1402.0553](#)].
- [48] N. Frusciante, M. Raveri, and A. Silvestri, *Effective Field Theory of Dark Energy: a Dynamical Analysis*, *JCAP* **1402** (2014) 026, [[arXiv:1310.6026](#)].
- [49] B. Hu, M. Raveri, N. Frusciante, and A. Silvestri, *Effective Field Theory of Cosmic Acceleration: an implementation in CAMB*, *Phys. Rev.* **D89** (2014), no. 10 103530, [[arXiv:1312.5742](#)].
- [50] M. Raveri, B. Hu, N. Frusciante, and A. Silvestri, *Effective Field Theory of Cosmic Acceleration: constraining dark energy with CMB data*, *Phys. Rev.* **D90** (2014), no. 4 043513, [[arXiv:1405.1022](#)].
- [51] N. Frusciante, G. Papadomanolakis, and A. Silvestri, *An Extended action for the effective field theory of dark energy: a stability analysis and a complete guide to the mapping at the basis of EFTCAMB*, [arXiv:1601.0406](#).
- [52] J. Gleyzes, D. Langlois, F. Piazza, and F. Vernizzi, *Exploring gravitational theories beyond Horndeski*, *JCAP* **1502** (2015) 018, [[arXiv:1408.1952](#)].
- [53] J. Gleyzes, D. Langlois, and F. Vernizzi, *A unifying description of dark energy*, *Int. J. Mod. Phys.* **D23** (2015), no. 13 1443010, [[arXiv:1411.3712](#)].
- [54] J. Gleyzes, D. Langlois, M. Mancarella, and F. Vernizzi, *Effective Theory of Interacting Dark Energy*, *JCAP* **1508** (2015), no. 08 054, [[arXiv:1504.0548](#)].
- [55] J. Gleyzes, D. Langlois, M. Mancarella, and F. Vernizzi, *Effective Theory of Dark Energy at Redshift Survey Scales*, *JCAP* **1602** (2016), no. 02 056, [[arXiv:1509.0219](#)].
- [56] G. D’Amico, Z. Huang, M. Mancarella, and F. Vernizzi, *Weakening Gravity on Redshift-Survey Scales with Kinetic Matter Mixing*, [arXiv:1609.0127](#).
- [57] **Planck** Collaboration, P. A. R. Ade et al., *Planck 2013 results. XVI. Cosmological parameters*, *Astron. Astrophys.* **571** (2014) A16, [[arXiv:1303.5076](#)].
- [58] J. Noller, F. von Braun-Bates, and P. G. Ferreira, *Relativistic scalar fields and the quasistatic approximation in theories of modified gravity*, *Phys. Rev.* **D89** (2014), no. 2 023521, [[arXiv:1310.3266](#)].
- [59] I. Sawicki and E. Bellini, *Limits of quasistatic approximation in modified-gravity cosmologies*, *Phys. Rev.* **D92** (2015), no. 8 084061, [[arXiv:1503.0683](#)].
- [60] A. Adams, N. Arkani-Hamed, S. Dubovsky, A. Nicolis, and R. Rattazzi, *Causality, analyticity and an IR obstruction to UV completion*, *JHEP* **10** (2006) 014, [[hep-th/0602178](#)].
- [61] J. B. Jiménez, F. Piazza, and H. Velten, *Piercing the Vainshtein screen with anomalous gravitational wave speed: Constraints on modified gravity from binary pulsars*, [arXiv:1507.0504](#).
- [62] S. Tsujikawa, *Possibility of realizing weak gravity in redshift space distortion measurements*, *Phys. Rev.* **D92** (2015), no. 4 044029, [[arXiv:1505.0245](#)].
- [63] E. J. Ruiz and D. Huterer, *Testing the dark energy consistency with geometry and growth*, *Phys. Rev.* **D91** (2015) 063009, [[arXiv:1410.5832](#)].

- [64] M. Kunz, S. Nesseris, and I. Sawicki, *Using dark energy to suppress power at small scales*, *Phys. Rev. D* **D92** (2015), no. 6 063006, [[arXiv:1507.0148](#)].
- [65] J. L. Bernal, L. Verde, and A. J. Cuesta, *Parameter splitting in dark energy: is dark energy the same in the background and in the cosmic structures?*, *JCAP* **1602** (2016), no. 02 059, [[arXiv:1511.0304](#)].
- [66] H. Steigerwald, *Probing non-standard gravity with the growth index of cosmological perturbations*, *PoS FFP14* (2016) 098.
- [67] T. Okumura et al., *The Subaru FMOS galaxy redshift survey (FastSound). IV. New constraint on gravity theory from redshift space distortions at $z \sim 1.4$* , *Publ. Astron. Soc. Jap.* **68** (2016) 47, [[arXiv:1511.0808](#)].
- [68] V. Salvatelli, F. Piazza, and C. Marinoni, *Constraints on modified gravity from Planck 2015: when the health of your theory makes the difference*, [arXiv:1602.0828](#).
- [69] A. Nishizawa and T. Nakamura, *Measuring Speed of Gravitational Waves by Observations of Photons and Neutrinos from Compact Binary Mergers and Supernovae*, *Phys. Rev. D* **D90** (2014), no. 4 044048, [[arXiv:1406.5544](#)].
- [70] E. Bellini and I. Sawicki, *Maximal freedom at minimum cost: linear large-scale structure in general modifications of gravity*, *JCAP* **1407** (2014) 050, [[arXiv:1404.3713](#)].
- [71] E. Bellini, R. Jimenez, and L. Verde, *Signatures of Horndeski gravity on the Dark Matter Bispectrum*, *JCAP* **1505** (2015), no. 05 057, [[arXiv:1504.0434](#)].
- [72] E. Bellini, A. J. Cuesta, R. Jimenez, and L. Verde, *Constraints on deviations from Λ CDM within Horndeski gravity*, [arXiv:1509.0781](#).
- [73] **Planck** Collaboration, P. A. R. Ade et al., *Planck 2015 results. XIV. Dark energy and modified gravity*, [arXiv:1502.0159](#).
- [74] J. Gleyzes, D. Langlois, F. Piazza, and F. Vernizzi, *Healthy theories beyond Horndeski*, *Phys. Rev. Lett.* **114** (2015), no. 21 211101, [[arXiv:1404.6495](#)].